WILEY

Modelling of snow interception on a Japanese cedar canopy based on weighing tree experiment in a warm winter region

Takafumi Katsushima[1] | Akio Kato[2] | Hideharu Aiura[3] | Kazuki Nanko[4] | Satoru Suzuki[5] | Yukari Takeuchi[1] | Shigeki Murakami[6]

[1]Tohkamachi Experimental Station, Department of Disaster Prevention, Meteorology and Hydrology, Forestry and Forest Products Research Institute, Tokamachi, Niigata, Japan

[2]Vocational Training Section for Forestry Workers, Toyama Prefecture Agriculture, Forestry and Fisheries Public Corporation, Tateyama, Toyama, Japan

[3]Forestry Research Institute, Toyama Prefectural Agricultural, Forestry and Fisheries Research Center, Tateyama, Toyama, Japan

[4]Department of Disaster Prevention, Meteorology and Hydrology, Forestry and Forest Products Research Institute, Tsukuba, Ibaraki, Japan

[5]Center for Forest Damage and Risk Management, Forestry and Forest Products Research Institute, Tsukuba, Ibaraki, Japan

[6]Kyushu Research Center, Forestry and Forest Products Research Institute, Kumamoto, Japan

Correspondence
Takafumi Katsushima, Tohkamachi Experimental Station, Forestry and Forest Products Research Institute, 614-9 Kawaharacho, Tokamachi, Niigata 948-0013, Japan.
Email: katusima@affrc.go.jp

Abstract

Snow interception by tree canopy affects the water and energy budgets. Several snow interception models have been proposed to estimate the temporal change of intercepted snow on the tree canopy from meteorological data. However, most models are based on a few observational results at limited sites or some conceptual understandings and assumptions; they still need more observational evidence and more detailed descriptions in the parameterization model for snow accumulation and snow unloading response to various meteorological conditions. A weighing tree experiment that measures the intercepted snow on the cut Japanese cedar trees was conducted in Tokamachi, Japan, to investigate the relationship between meteorological conditions and the change of intercepted snow. The results showed that the interception efficiency, which shows the ratio of intercepted snow to the total precipitation, increased with increasing air temperature in the range from -4.2 to $0°C$ due to increased adhesion and cohesion of snow. The maximum interception capacity was not present in observations such as an air temperature range. The unloading of intercepted snow from the canopy induced by snowmelt was related to air temperature, solar radiation, and intercepted snow amount. The snow unloading caused by wind-blowing intercepted snow off the tree, started to develop at wind speeds exceeding 0.8 m s^{-1}. The wind-induced snow unloading rate coefficient increased as the wind speed increased. This study proposed a new parameterization model of snow interception based on these observations. It is the only snow interception model to use solar radiation in the snow unloading parameterization. It found that simulated and observed temporal changes of intercepted snow correlated well. Nevertheless, there were significant errors between the simulated and observed intercepted snow on several snowfall events because the model could not accurately assess the occurrence of snow unloading due to snowmelt.

KEYWORDS
snow, canopy, interception, accumulation, unloading, modelling

1 | INTRODUCTION

Snowfall in the forest is partially intercepted by the canopy. Snowfall interception can reduce the amount of subcanopy snow by increasing sublimation of intercepted snow (Lundberg & Halldin, 1994; Nakai et al., 1994; Schmidt, 1991) and meltwater drip from intercepted snow (Storck et al., 2002). The intercepted snow also increases albedo at the land surface (Betts & Ball, 1997). Snowfall interception affects the water and energy budgets in areas where snowfall occurs.

To demonstrate and model the behaviour of snow on the tree canopy, the weighing tree experiments that measure intercepted snow by measuring the change in weight of the entire cut tree have been conducted at several sites. Satterlund and Haupt (1967) showed that intercepted snow increases as the cumulative snowfall precipitation grow, and it asymptotically approaches the maximum values of intercepted snow, known as 'maximum interception capacity' that can be stored on the canopy. Based on the concept of maximum interception capacity, the relationship between intercepted snow and cumulative snowfall precipitation was modelled using a sigmoid curve (Moeser et al., 2015; Satterlund & Haupt, 1967; Schmidt & Gluns, 1991) or an exponential curve (Hedstrom & Pomeroy, 1998). On the other hand, Storck et al. (2002) found that the intercepted snow increased linearly with the increase in cumulative snowfall precipitation. The maximum interception capacity did not appear in a warmer region, even though the range of intercepted snow and cumulative snowfall precipitation was much greater than that observed by Satterlund and Haupt (1967) and Schmidt and Gluns (1991). The difference in the form of these functions induces a significant difference in the amount of intercepted snow, especially when the event total snowfall precipitation is large. Therefore, the function form and model parameters must be chosen carefully.

The maximum interception may vary depending on meteorological conditions, such as air temperature and wind speed. Schmidt and Gluns (1991) demonstrated that the maximum interception capacity is inversely proportional to the density of new snow. Hedstrom and Pomeroy (1998) developed an interception model based on a study by Schmidt and Gluns (1991). The maximum interception capacity was modelled as a function of leaf area index (LAI) and new snow density. This model assumed a relationship in which the maximum interception capacity decreased with increasing air temperature. However, other research displayed snow cohesion and adhesion increase when the air temperature is $>-3°C$. As a result, snow accumulation on a narrow board increases with increasing air temperature (Kobayashi, 1987; Pfister & Schneebeli, 1999; Takahashi & Takahashi, 1952). Some models implement a parameterization model which expresses increasing the maximum interception capacity due to increasing air temperature (Andreadis et al., 2009; Lundquist et al., 2021; Roth & Nolin, 2019). Lundquist et al. (2021) suggested the need for its implementation. However, the response to increasing air temperature employed in these models is the opposite of the model parameterization developed by Hedstrom and Pomeroy (1998). Takahashi (1952) found that interception efficiency, which is the ratio of intercepted snow to snowfall precipitation, increases when air temperature ranges from -3 to $0°C$. This suggests that the maximum interception capacity may also increase with increasing air temperatures. Although such observed data had been obtained during the initial study of snow interception, they were not formulated and were not adopted in subsequent models. Therefore, the behaviour of snow interception to changes in meteorological conditions remains partially unknown.

Accurate estimates of the amount of intercepted snow necessitates a thorough understanding of both the response of snow accumulation and unloading phenomena to meteorological conditions. In colder continental climates, sublimation is a dominant process for intercepted snow unloading, and in warmer maritime climates, mechanical removal due to snowmelt and meltwater drip are the dominant processes (Lundquist et al., 2021). Mechanical removal has been expressed as a function of air temperature and/or wind speed, and the function has not considered solar radiation (Gregow et al., 2008; Liston & Elder, 2006; Roesch et al., 2001). Model parameters were determined based on certain conceptual understandings and assumptions (Miller, 1966; Nakai et al., 1994; Yamazaki et al., 1996). Takahashi (1952) demonstrated from measured data that intercepted snow is quickly unloaded through melt effects from solar radiation and sensible heat at air temperatures greater than $0°C$. At wind speeds $>1 \text{ m s}^{-1}$ and air temperatures less than $0°C$, snow unloading increases with increasing wind speed. However, these findings have not been developed and integrated into the model. There is a possibility that knowledge of the response of snow accumulation and snow unloading to meteorological conditions based on observational results may be insufficient to accurately estimate the behaviour of intercepted snow.

Based on studies of the difference in the event based snowfall depth differences between the forest and open sites, it has been demonstrated that interception efficiency and its variability are related to the forest canopy structure (Moeser et al., 2015; Roth & Nolin, 2019). Those results allowed for the modelling of the spatial variability of snow interception caused by the structure of the forest canopy (Helbig et al., 2020; Moeser et al., 2016). However, these observations only provide event-based data and cannot measure changes in intercepted snow during a snowfall event or snow unloading following an event. Despite not being able to show the relationship between snow interception and forest canopy structure, traditional weighing tree experiments can be used to investigate the relationship between meteorological conditions and the behaviour of intercepted snow.

This study presented a novel parameterization model of intercepted snow, named the Japanese cedar snow interception model (JSIM), based on the findings of the analysed snow accumulation and unloading. This study aims to (1) investigate the relationship between meteorological conditions and the behaviour of intercepted snow on the tree canopy through direct measurements of intercepted snow on the tree canopy and (2) propose a new model for snow interception and unloading, that integrates meteorological data. A weighing tree experiment using cut Japanese cedar trees (*Cryptomeria japonica*) was conducted to directly observe the amount of intercepted snow over four snow seasons in a warm and heavy snow environment in Japan. This study analysed the response of snow accumulation and unloading to temperature, wind speed, and solar radiation. The effects of the forest canopy structure and density, such as canopy gap, canopy height, and LAI, were not analysed in this study.

2 | METHODS

2.1 | Weighing tree experiment

This experiment was conducted at the Tohkamachi experimental station (37°07.9′ N, 138°46.0′ E, 200 m a.s.l.) of the Forest and Forestry Product Research Institute (FFPRI) for four seasons from 2016–2017 to 2019–2020. The abovementioned study by Takahashi (1952) was carried out at this same site. The site is located in Tokamachi, Japan, a low-elevation mountainous area in central Japan facing the Japan Sea. We observed the amount of intercepted snow on a cut tree in an open area for meteorological observation. Figure 1 shows a schematic of the measurement apparatus. We used a similar design from previous studies conducted by Takahashi (1952) and Kato (2000). Four flat concrete plates were placed on the ground and four load cells (Kyowa Co., LCN-A-5KN) were placed on top of these. A mount with a 16-cm inner sleeve was placed on these load cells to hold the tree. The load cells were positioned on the four corners of the mount. The cut tree was set using a crane into the inner sleeve of the mount. Anchor piles were inserted through the holes in the bottom of the mount to prevent it from tipping over due to wind. The apparatus was covered with wooden boards to prevent snow from accumulating on the
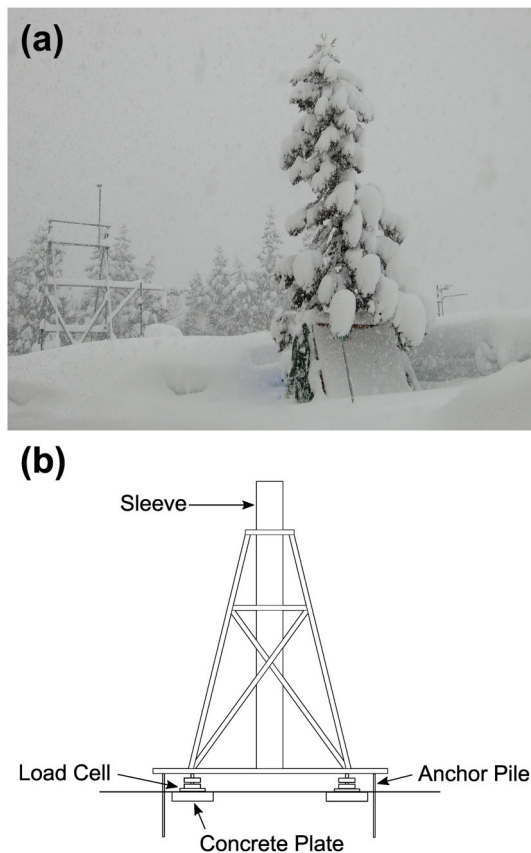

FIGURE 1 (a) Photograph of intercepted snow on the cut tree taken on 13 February 2018, at Tokamachi, Japan representing a 15-mm snow load on the Japanese cedar canopy. (b) Schematic of measurement apparatus.

mount. The snow around the apparatus was occasionally removed to prevent the branches from contacting the snowpack surface. The force applied to each load cell was recorded by a data logger (Kyowa Co., UCAM-60B) at 10-min intervals and a resolution of 1.25 N. After the cut-tree was set on the mount, the measured total force at this time was set as the correction value, and differences in total force from the correction value were recorded in subsequent measurements. The amount intercepted snow of the whole tree was obtained from the changes in measured force. The intercepted snow was expressed as the unit of snow water equivalent in millimetres for the vertical projection area of the tree canopy. When the measured intercepted snow had a negative value due to the drying of the cut-tree, the correction value was updated before the next snowfall event began. Table 1 shows the properties of the cut-trees used each snow season. The top of the Japanese cedar trees, which was about 6–7 m high, was used for the measurements. Different tree tops were taken each winter from the same forest near the observation site, where the trees are about 40 years old and 12 m tall. The tree tops were transported by a truck. Assuming that the vertical projection of tree crowns was circular, the vertical projection crown area was obtained from the average of the canopy radii measured in eight directions.

2.2 | Meteorological observations

Meteorological observations were conducted in the same open area as the weighing tree experiment. Air temperature (Yokogawa Electric Co., E-734) was automatically measured at 4 m above the ground, wind speed (Sonic Co., SAT-540H) at 10.5 m above the ground, and downward shortwave radiation (Eko Instrument Co., MS-402F) at 4.3 m above the ground. Hourly precipitation rate was observed using the SR2A precipitation gauge (Tamura, 1993), which has a resolution of 0.005 mm. The precipitation gauge was placed inside a wind fence 4 m high and 3 m above the ground. For backup observation of precipitation, we used the Japanese standard precipitation gauge RT-4 (Yokogawa Electric Co., B-071) at 3 m above the ground.

The precipitation gauge displayed an undercatch of snowfall induced by the wind; therefore, adjustment of precipitation measurements was necessary to obtain the true precipitation amount (Goodison et al., 1998). The measured precipitation was calibrated by following Equation (1) of the catch ratio CR proposed by Yoshida and Saito (1956):

$$CR = \frac{1}{1 - m\, u_G}, \tag{1}$$

where, m is a coefficient that depends on the gauge type and precipitation type and u_G is wind speed (m s^{-1}) at the height of the gauge opening. For calibration, we used $m = 0.6$ and $m = 0.26$ for dry and wet snow, respectively. These coefficient values were obtained from a comparison between the measured precipitation by SR2A and the Double Fence Intercomparison Reference (Masuda et al., 2018). Moreover, $m = 0.128$ was used to calibrate of precipitation rate observed by RT-4 (Yokoyama et al., 2003). We estimated the wind

Snow season	Tree height (m)	Crown length (m)	Vertical projection crown area (m^2)
2016–2017	6.8	4.5	3.2
2017–2018	6.1	3.6	7.0
2018–2019	6.0	3.6	5.0
2019–2020	6.0	3.6	5.5

TABLE 1 Tree height, crown length, and vertical projection crown area used in the study.

speed at the height of the precipitation gauge opening using Equation (2) of the log wind profile assumption:

$$u_G = u_H \frac{\log\left(\frac{h_G - HS}{z_0}\right)}{\log\left(\frac{H - HS}{z_0}\right)}, \quad (2)$$

where, u_H is the measured wind speed (m s^{-1}), h_G is the height of gauge opening (m), HS is the snow depth (m), H is the height of the anemometer (m), and z_0 is the aerodynamic roughness length (m). The depth of the snow was observed by using an ultrasonic snow depth sensor (Sonic Co., SL-350). We also used $z_0 = 0.005$ m as a representative value of the roughness of the land surface covered with snow (Davenport et al., 2000).

The wind speed at one-third of the canopy length, which corresponds to the centre of gravity when the horizontal projection of the canopy is assumed to be a triangle, was used as the wind speed to describe the behaviour of intercepted snow against the wind in the analysis and the interception model. This wind speed was estimated by Equation (2), replacing the height of the gauge opening with this height.

2.3 | Analysis of snow interception

The temporal change in the intercepted snow is represented by the following components shown in Equation (3):

$$\frac{dI}{dt} = L - U - M - S, \quad (3)$$

where, I is the intercepted snow per unit vertical projection area of the canopy in units of snow water equivalent (mm), L is the snow loading rate (mm h^{-1}), U is the snow unloading rate due to snow melt and wind (mm h^{-1}), M is the unloading rate due to the drip of snow melting water (mm h^{-1}), and S is the sublimation rate (mm h^{-1}). This equation is a fundamental formula used by many snow interception models (Lundquist et al., 2021). The equation ignored the process of riming, which increases the intercepted snow independent of precipitation falling and affects wind-induced snow unloading (Lumbrazo et al., 2022). The difference between M and U is that M is dripping off liquid water producing due to snow melt, and U is slipping off intercepted snow due to snow melt or wind.

Snowmelt occurs when the air temperature is greater than 0°C, but under these conditions, the snow unloading due to drip off of snow melting water is also significant. Whether the intercepted snow is removed as snow or snow melting water affects the snow accumulation

beneath the forest canopy (Storck et al., 2002). Distinguishing between these in snow interception models will lead to improved modelling of forest snowpack. However, it is not easy to separate the amount of the snow unloading rate due to snow melt and the drip of snow melting water from our observations. Then, the unloading rate due to the drip of snow melting water in Equation (3) was not explicitly described but was included in the snow unloading rate due to snow melt and wind. Furthermore, sublimation increases as wind velocity increases (Lundberg & Halldin, 1994; Nakai et al., 1994), but under this condition, the snow unloading due to wind is also expected to increase. Even if we observe the behaviour of decreasing intercepted snow with increasing wind speed, for the same reason, it is not easy to separate the amount of the snow unloading rate due to wind and the sublimation from our observations. Then, sublimation in Equation (3) was also included in the snow unloading rate due to snow melt and wind.

The snow loading rate and the snow unloading rate can be simply shown by the following equations, respectively:

$$L = \frac{dI}{dP} p, \quad (4)$$

$$U = fI, \quad (5)$$

where, $\frac{dI}{dP}$ is the interception efficiency, P is the total precipitation (mm), p is the precipitation rate (mm h^{-1}), and f is the snow unloading rate coefficient for 1 h (h^{-1}). As mentioned above, interception efficiency is a function of the maximum interception capacity (Satterlund & Haupt, 1967). The maximum interception capacity was obtained by gathering several data on intercepted snow and event total precipitation obtained immediately after storm events. Snow unloading can occur during storm events; however, it is not possible to determine from the data whether it occurred. Therefore, the maximum interception capacity may include snow unloading during storm events that cannot be explicitly stated. At the experimental site, air temperatures during snowfall are near 0°C, snow unloading due to snowmelt is likely to occur even during snowfall. Thus, we did not measure the maximum interception capacity; rather, we measured the interception efficiency at each time. In prior studies, snow unloading from snowmelt and snow unloading from wind have been parameterized as unique functions (Lundquist et al., 2021; Roesch et al., 2001). In accordance with these previous studies, snow unloading due to snowmelt f_{melt} (h^{-1}) and wind f_{wind} (h^{-1}) were obtained separately.

$\frac{dI}{dP}$ and f were obtained from the change in observed intercepted snow amount in 1 h and precipitation rate by the following Equations (6) and (7):

$$\frac{dI}{dP} = \frac{I_n - I_{n-1}}{p_n}, \tag{6}$$

$$f = -\frac{I_n - I_{n-1}}{I_{n-1}}, \tag{7}$$

where, I_n and I_{n-1} are the intercepted snow (mm) for each time point and p_n is the precipitation rate (mm h^{-1}).

The interception efficiency was determined from the data when we observed an increase in intercepted snow and a precipitation rate of 1 mm h^{-1} or greater. Precipitation types such as snow or rain are related to air temperature, and a past observation at the Tohkamachi experimental station showed that the frequency ratio of snowfall was 50% at a temperature of 1.5°C (Takeuchi et al., 2016). Moreover, snow unloading due to snowmelt is more likely to occur during the daytime, and snow unloading due to wind occurs when wind speed is >1 m s^{-1} (Takahashi, 1952). Therefore, to obtain the interception efficiency, we used only the data gathered during the nighttime with a wind speed of ≤1 m s^{-1} and air temperature of ≤1.5°C. The snow unloading rate coefficient f was determined from the data when we observed a decrease in intercepted snow with an intercepted snow amount of ≥5 mm and no precipitation. f_{melt} was obtained using data obtained during the daytime with wind speeds of ≤1 m s^{-1}. f_{wind} was obtained from nighttime data with an air temperature of <0°C which snowmelt is negligible.

2.4 | Multiple linear regression analysis

We analysed the relation for the coefficient of $\frac{dI}{dP}$, f_{melt}, and f_{wind} to mereological condition using the multiple linear regression analysis to make a parameterization model of each coefficient in JSIM. Air temperature, wind speed, and intercepted snow were used as potential explanatory variables in the analysis of $\frac{dI}{dP}$. The p-value of each variable, coefficient of determination R^2, and Akaike Information Criterion (AIC) of all seven possible regression equations with the combination of three variables were determined. The regression equation for the combinations of explanatory variables that consists only of statistically significant variables ($p < 0.05$) and minimizes the AIC was selected as the best regression equation from these seven equations. The root mean square error (RMSE) between the measured and modelled η was also determined to quantify the accuracy of the best regression equation. Previous studies demonstrated a relationship between the air temperature and the interception efficiency when the air temperature is <0°C and no relationship when it is >0°C (Takahashi, 1952). Because the relationship of the interception efficiency to air temperature is likely to be different for temperatures above and below 0°C; therefore, the analysis of $\frac{dI}{dP}$ was conducted separately for air temperatures of 0°C or more and those less than 0°C.

Air temperature, solar radiation, and the amount of intercepted snow were used as potential explanatory variables for f_{melt}. The best regression equation for f_{melt} was selected using the same procedure with the analysis of $\frac{dI}{dP}$ from the seven possible regression equations

with the combination of these three variables. The intercept of the regression model for f_{melt} was forced to zero because the unloading rate is assumed to be zero under conditions where the air temperature is 0°C, no solar radiation occurs and no intercepted snow is present. The regression model for f_{wind} only considers wind speed as an explanatory variable, and the intercept of its model was also forced to zero. RMSE between the measured and modelled f_{melt}, and f_{wind} were determined to quantify their accuracy.

2.5 | Modelling of snow interception

We formulated an equation for determining the time change of intercepted snow in JSIM as Equation (8).

$$\frac{dI}{dt} = \frac{dI}{dP}p - (f_{melt} + f_{wind})I. \tag{8}$$

We made a parameterization model to determine each coefficient of $\frac{dI}{dP}$, f_{melt}, and f_{wind} in JSIM as a function of mereological variables based on multiple linear regression analysis results. The time series of intercepted snow was simulated from the observed meteorological data using Equation (8) and parameterized $\frac{dI}{dP}$, f_{melt}, and f_{wind}. We analysed the relation between the measured and modelled snow interception. We used the correlation coefficient r between these data, the mean error (ME), and the RMSE to validate the developed model.

2.6 | Model intercomparison

We validated the performance of JSIM and discussed the adequate models to represent snow interception phenomena in warmer regions through an intercomparison of simulated results by the JSIM and other models. The intercomparison of the simulated results of the time series of intercepted snow between JSIM and previously developed models was conducted to validate the performance of JSIM. We compared the changes in the time series when the snow interception or the snow unloading parameterization model in JSIM were replaced with those employed in other models, respectively.

2.6.1 | Intercomparison of snow interception parameterization

Three models were selected as a snow interception parameterization for model intercomparison. The first model of snow interception is a model for the boreal forest developed by Hedstrom and Pomeroy (1998). It assumes an exponential curve of intercepted snow to maximum interception capacity with increasing cumulative snowfall precipitation, and the following equation expresses the interception efficiency:

$$\frac{dI}{dP} = k(I_{max} - I_0 - I),\tag{9}$$

where, k is the proportionality factor, I_{max} is the maximum interception capacity, and I_0 is the initial interception. $k = 1/I_{max}$ was adopted based on a suggestion by Hedstrom and Pomeroy (1998), and I_0 was set to zero. I_{max} was estimated from the following equations of LAI and new snow density:

$$I_{max} = \bar{I}\left(0.27 + \frac{46}{\rho_s}\right)\text{LAI},\tag{10}$$

where, $\bar{I}$ is the maximum interception capacity on the tree branch. $\bar{I} = 6.6$ (mm) for pine obtained by Schmidt and Gluns (1991) and LAI $= 4.1$ (m^2 m^{-2}) for the black spruce stand used in the experiment by Hedstrom and Pomeroy (1998) were used. New snow density was estimated from the following relation of air temperature.

$$\rho_s = 67.92 + 51.25 e^{(T_a/2.59)}.\tag{11}$$

From Equations (10) and (11), Hedstrom and Pomeroy (1998) assume that maximum interception capacity decreases with increasing air temperature.

Second, the equation of maximum interception capacity in Equation (9) was changed to the following Equation (12) by Lundquist et al. (2021), assuming that maximum interception capacity increases at an air temperature of $>-3°$C due to increased adhesion and cohesion of snow.

$$I_{max} = \begin{cases} 85, & T_a > 0°\text{C} \\ (63/3)(T_a + 3) + 20, & -3°\text{C} < T_a \leq 0°\text{C}. \\ 20, & T_a \leq -3°\text{C} \end{cases}\tag{12}$$

The parameterization adopts the opposite behaviour to the relationship of maximum interception capacity to air temperature assumed in Equations (10) and (11) by Hedstrom and Pomeroy (1998).

The third model was based on the assumption that intercepted snow increases at a constant interception efficiency until maximum interception capacity (Storck, 2000).

$$\frac{dI}{dP} = \begin{cases} 0.6, & I < I_{max} \\ 0.0, & I = I_{max} \end{cases}.\tag{13}$$

The following Equations (14) and (15) by Andreadis et al. (2009), which modified the equation of maximum interception capacity in Storck (2000), was used:

$$I_{max} = L_r(m \times \text{LAI}),\tag{14}$$

$$L_r = \begin{cases} 4.0, & T_a > -1°\text{C} \\ 1.5T_a + 5.5, & -3°\text{C} < T_a \leq -1°\text{C}, \\ 1.0, & T_a \leq -3°\text{C} \end{cases}\tag{15}$$

where, L_r is the leaf area ratio, and m is the empirical constant. $m \times \text{LAI} = 10.0$ was used according to the parameter setting of Storck (2000).

2.6.2 | Intercomparison of snow unloading parameterization

Two models were selected as snow unloading parameterization for model intercomparison. The first model is a parameterization model for boreal forests developed by Hedstrom and Pomeroy (1998), which assumes that intercepted snow decreases exponentially over time and does not separately describe sublimation, snow unloading due to snow melt and wind, or meltwater dripping off. The following snow unloading rate coefficient proposed by Mahat and Tarboton (2014), based on estimated results of the decrease in intercepted snow with time by Hedstrom and Pomeroy (1998), was used for intercomparison.

$$f = 0.00463.\tag{16}$$

The second model is a parameterization model developed by Roesch et al. (2001), which has parameterized the snow unloading rate coefficient due to snow melt and wind:

$$f = f(T_a) + f(u),\tag{17}$$

$$f(T_a) = \begin{cases} \frac{3600(3.0 + T_a)}{1.87 \times 10^5} = 0.0193(3.0 + T_a), & T_a > -3°\text{C} \\ 0.0, & T_a \leq -3°\text{C} \end{cases},\tag{18}$$

$$f(u) = \frac{3600}{1.56 \times 10^5}u = 0.0231u,\tag{19}$$

where, $f(T_a)$ is the snow unloading rate coefficient due to snow melt as a function of air temperature, and $f(u)$ is the snow unloading rate coefficient due to wind.

3 | RESULTS

3.1 | Weighing tree experiment and meteorological observation

Figure 2 shows the observed results of intercepted snow I and air temperature T_a for each studied snow season. The period shown in grey in these figures indicates the period, during which there are missing data of precipitation rate observed using a precipitation gauge of SR2A due to equipment malfunction. The data observed during this period were not used to analyse the coefficients of $\frac{dI}{dP}$, f_{melt}, and f_{wind}. From Figure 2, the intercepted snow repeatedly increased and decreased over a short time. The duration of the
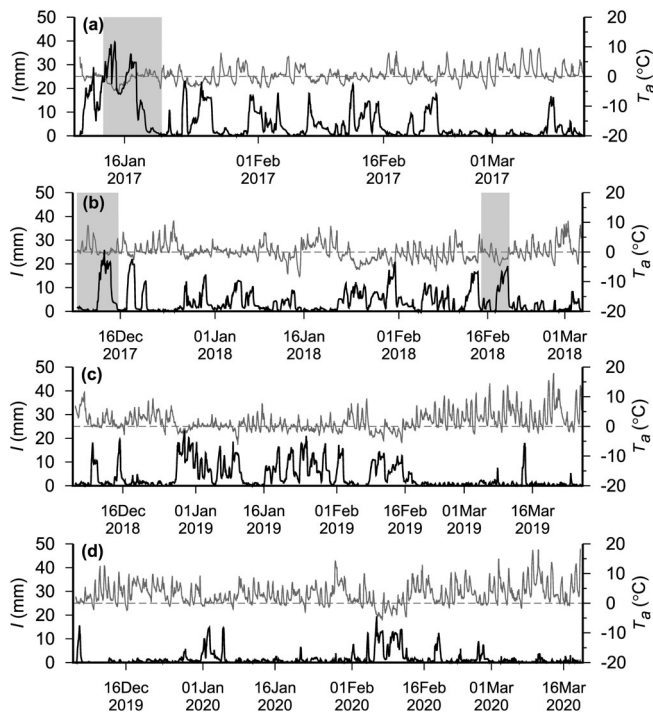
FIGURE 2 Time series of hourly variation of (a) intercepted snow I and air temperature T_a for 2016–2017, (b) for 2017–2018, (c) for 2018–2019, and (d) for 2019–2020. Black line showed intercepted snow and grey line showed air temperature. Periods shaded in grey indicate periods when precipitation was observed by a backup precipitation gauge due to equipment malfunction.

existing intercepted snow on the tree canopy was a few days for most snow interception events and 1 week at the longest. The intercepted snow decreased and approached zero after temperatures began to exceed 0°C for most snow interception events. The maximum intercepted snow value in the four snow seasons was 40 mm, which was observed on 14 January 2017. However, most of the maximum values of intercepted snow for each snow event ranged from 10 to 20 mm.

3.2 | Interception efficiency

Figure 3 shows the observed interception efficiency $\frac{dI}{dP}$ against air temperature T_a (Figure 3a), intercepted snow I for air temperature ≥0°C (Figure 3b), wind speed u for air temperature ≥0°C (Figure 3c), intercepted snow I for air temperatures <0°C (Figure 3d), and wind speed u for air temperatures <0°C (Figure 3e). Table 2 shows the results of multiple linear regression analysis for seven possible regression equations with the combinations of three potential explanatory variables of T_a, I, and u. The values in the table show the estimated intercept term, the estimated regression coefficients for each explanatory variable, R^2, and AIC for each regression equation. The p-value of each variable was shown as significant codes in the coefficient for the variable in the table. The numbers in bold show the best regression model obtained by the best subset selection procedure. Data of interception efficiency were obtained at air

temperatures ranging from −4.2 to 1.3°C, with most of them near 0°C. The observed interception efficiency ranged from 0.02 to 1.33, and values >1 were obtained for some of the data. The mean value interception efficiency was 0.54 ($N = 144$) for air temperatures of ≥0°C and 0.63 ($N = 190$) for air temperatures <0°C. Interception efficiency tends to decrease with increasing air temperature ≥0°C and tends to increase with increasing air temperature at <0°C (Figure 3a). The mean value of interception efficiency increased from 0.31 to 0.57 about two times when air temperature increased from −4 to −3°C. For air temperature ≥0°C, the interception efficiency when intercepted snow ranged between 5 and 10 mm was greater than when intercepted snow was above or below this range (Figure 3b). For air temperature <0°C, the interception efficiency did not change with increasing intercepted snow (Figure 3d). The interception efficiency tended to decrease with increasing wind speed for both temperature conditions (Figure 3c,e).

From the linear regression analysis results with a single explanatory variable and intercepted term shown in Table 2, the estimated regression coefficient on air temperature was −0.54 for air temperature ≥0°C and 0.062 for air temperature <0°C. That trends were statistically significant ($p < 0.001$) for both air temperature conditions. The linear regression analysis also showed no statistically significant relation between the interception efficiency and the amount of intercepted snow under both temperature conditions ($p ≥ 0.05$). The estimated regression coefficient on wind speed was −0.23 for air temperature ≥0°C and −0.21 for air temperature <0°C. There were both found to be statistically significant ($p < 0.01$).

The results of the multiple regression analysis for air temperature ≥0°C showed that the best regression model was the one in that combined air temperature ($p < 0.001$) and intercepted snow ($p < 0.05$). For air temperature <0°C, the combination of air temperature ($p < 0.001$) and wind speed ($p < 0.001$) was shown to be the best regression model. The best regression model predicted interception efficiency with an R^2 of 0.38, AIC of −48.5 for air temperature ≥0°C and with R^2 of 0.16 and AIC of −49.9 for air temperatures <0°C.

Figure 4 shows the scatterplot between the measured and modelled interception efficiency. The RMSE between these data were RMSE = 0.20 for air temperature ≥0°C and RMSE = 0.21 for air temperature <0°C. When these best regression models for air temperature <0°C are used to predict the interception efficiency outside the range of the air temperature used in this analysis, the predicted interception efficiency can be less than zero. The interception efficiency is expected to be constant value at temperatures below −3°C in previous studies (Andreadis et al., 2009; Kobayashi, 1987; Lundquist et al., 2021). Based on such assumption and results of the multiple regression analysis, the following Equation (20) was employed to express the interception efficiency in Equation (8):

$$\frac{dI}{dP} = \begin{cases} 0.73 - 0.59T_a - 0.0082I, & T_a \geq 0°C \\ 0.86 + 0.064T_a - 0.22u, & -4°C \leq T_a < 0°C. \\ 0.86 + 0.064 \times (-4) - 0.22u, & T_a < -4°C \end{cases} \quad (20)$$
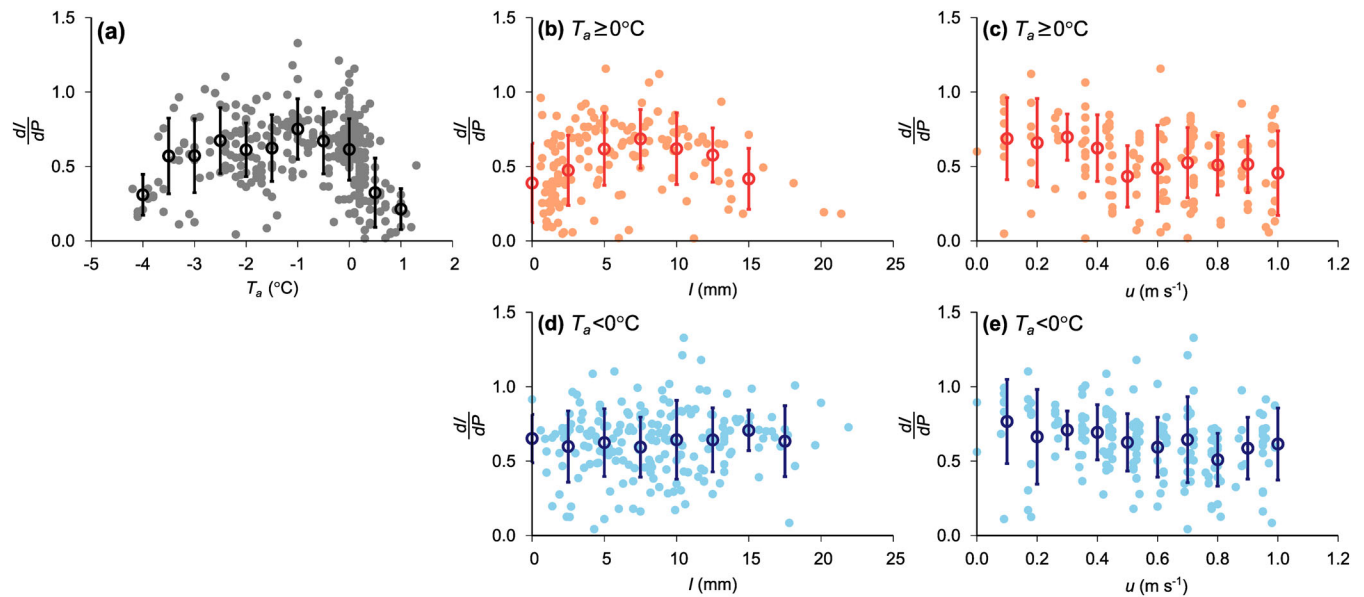
FIGURE 3 Scatterplot and binned scatterplots of interception efficiency $\frac{dI}{dP}$ against (a) air temperature T_a, (b) intercepted snow I at air temperatures $\geq 0°C$, (c) wind speed u at air temperatures $\geq 0°C$, (d) intercepted snow at air temperatures $T_a < 0°C$, and (e) wind speed u at air temperatures $< 0°C$. The open circles are the means of each bin, and the error bars represent the standard deviations. The data were obtained at night with a precipitation rate of $\geq 1\,mm\,h^{-1}$, a wind speed of $\leq 1\,m\,s^{-1}$, and an air temperature of $\leq 1.5°C$.

TABLE 2 Results of multiple regression analysis for all combinations of variables predicting interception efficiency $\frac{dI}{dP}$.

	Intercept	T_a	I	u	R^2	AIC
$T_a \geq 0°C$	0.67***	−0.54***	–	–	0.36	−46.4
	0.50***	–	0.0062[n.s.]	–	0.01	15.6
	0.68***	–	–	−0.23**	0.06	9.0
	0.73*	**−0.59***	**−0.0082*	–	**0.38	**−48.5
	0.73***	−0.52***	–	−0.12[n.s.]	0.37	−47.5
	0.65***	–	0.0041[n.s.]	−0.22*	0.06	10.3
	0.81***	−0.57***	−0.0090*	−0.13[n.s.]	0.39	−50.4
$T_a < 0°C$	0.73***	0.062***	–	–	0.10	−38.8
	0.59***	–	0.0048[n.s.]	–	0.01	−21.3
	0.75***	–	–	−0.21**	0.05	−30.1
	0.68***	0.063***	0.0057[n.s.]	–	0.11	−39.6
	0.86*	**0.064***	–	**−0.22***	**0.16	**−49.9
	0.72***	–	0.0037[n.s.]	−0.21***	0.06	−29.2
	0.82***	0.065***	0.0045[n.s.]	−0.22***	0.17	−49.8

Note: Estimated intercept term, the estimated regression coefficient for air temperature T_a, coefficient for intercepted snow I and coefficient for wind speed u, coefficient of determination (R^2), and AIC for each model. The numbers in bold indicate the best regression model. Significance codes: ***$p < 0.001$; **$p < 0.01$; *$p < 0.05$; [n.s.] Not significant.

3.3 | Snow unloading due to snowmelt

Figure 5 shows the relationship between the snow unloading rate coefficient due to snowmelt f_{melt} (h^{-1}) calculated using Equation (7) from the changes in the amount of intercepted snow for 1 h against air temperature T_a (°C) (Figure 5a), solar radiation $S^{\downarrow}$ ($MJ\,m^{-2}\,h^{-1}$) (Figure 5b), and the amount of intercepted snow I (mm) (Figure 5c). Table 3 shows the results of the multiple regression analysis with these data for all combinations of these three variables as explanatory

variables ($N = 103$). Snow unloading due to snowmelt was present in air temperatures that ranged between −3.7 and 3.5°C, and was close to 0 at temperatures $\leq -3°C$. The results of the linear regression analysis with a single explanatory variable shown in Table 3 indicate a statistically significant relationship between air temperature ($p < 0.001$), solar radiation ($p < 0.001$), and the amount of intercepted snow ($p < 0.001$) on f_{melt}. For all three variables, the estimated regression coefficient on these variables had a positive value. For solar radiation, the highest coefficient of determination and the lowest AIC was
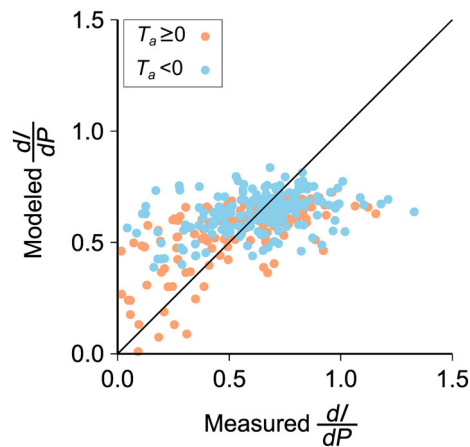
FIGURE 4 Comparison between modelled and measured interception efficiency $\frac{dI}{dP}$ for all four snow seasons. The solid line shows 1:1 relationship with a R^2 of 0.38, and RMSE of 0.20 at air temperatures ≥0°C and R^2 of 0.16, and RMSE of 0.21 for air temperatures <0°C.

TABLE 3 Results of multiple regression analysis for variables predicting the unloading rate coefficient due to snowmelt f_{melt}.

T_a	$S^{\downarrow}$	I	R^2	AIC
0.063***	–	–	0.23	−55.3
–	0.14***	–	0.72	−161.6
–	–	0.014***	0.44	−87.8
0.028***	0.13***	–	0.77	−175.9
0.068***	–	0.015***	0.69	−148.9
–	0.14***	−0.000059[n.s.]	0.72	−159.6
0.039*	**0.097***	**0.0049***	**0.78**	**−180.6**

Note: The estimated regression coefficient for air temperature T_a, coefficient for solar radiation $S^{\downarrow}$ and coefficient for intercepted snow I, coefficient of determination (R^2), and AIC for each model. The numbers in bold indicate the best regression model. Significance codes: ***$p < 0.001$; **$p < 0.01$; *$p < 0.05$; [n.s.] Not significant.

obtained compared with the other variables of air temperature or the amount of intercepted snow ($R^2 = 0.72$, AIC $= -161.6$). The model using all of these three variables was obtained as the best regression model from the results of multiple regression analysis. For the best regression model, both the coefficient of determination and the AIC was improved over the regression model with only solar radiation as a variable ($R^2 = 0.78$, AIC $= -180.6$). f_{melt} was formulated as the following Equation (21):

$$f_{melt} = 0.039\,T_a + 0.097\,S^{\downarrow} + 0.0049\,I. \tag{21}$$

3.4 | Snow unloading due to wind

Figure 6a shows the relationship between the snow unloading rates for 1 h due to wind U_{wind} (mm h^{-1}) and wind speed u (m s^{-1})
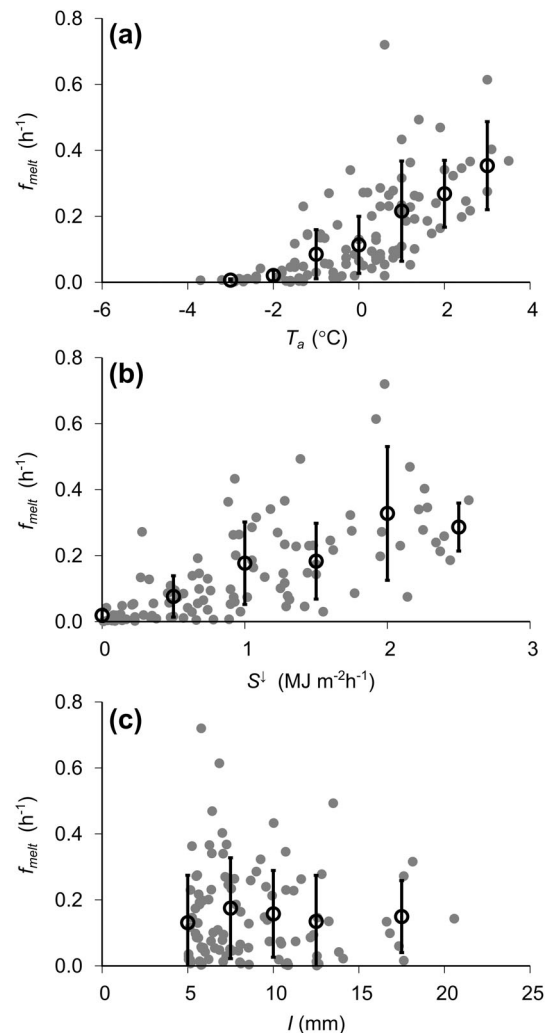

FIGURE 5 Scatterplot and binned scatterplot of snow unloading rate coefficients due to snowmelt f_{melt} against (a) air temperature T_a, (b) solar radiation $S^{\downarrow}$, and (c) intercepted snow I. The open circles indicate the means of each bin, and the error bars represent the standard deviations. The data were obtained during the day with an intercepted snow amount of ≥5 mm, a wind speed of ≤1 m s^{-1}, and no precipitation.

($N = 108$). As mentioned above, U_{wind} and f_{wind} includes the decrease in intercepted snow resulting from sublimation. The maximum sublimation rate from the intercepted snow in previous observational studies was 0.61 mm h^{-1} (Storck et al., 2002), which is shown as a dashed line in Figure 6a. From Figure 6a, most of the observed snow unloading rates were smaller than the maximum sublimation rates observed in previous studies. Only four data points exceeded these maximum sublimation rates, and they were clearly identifiable as the snow unloading due to wind. The smallest wind speed data among these four data was 0.8 m s^{-1}, and it showed that the snow unloading due to wind is possible to occur at least above this wind speed. Figure 6b shows the relationship between the snow unloading rate coefficient due to wind f_{wind} (h^{-1}) and wind speed. From Figure 6b, most of the observed snow unloading rate coefficients due to wind were less than
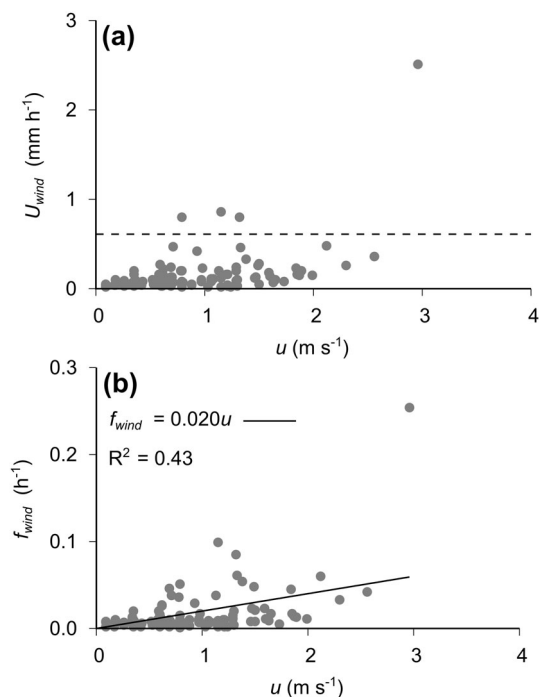
FIGURE 6 Scatterplot of (a) snow unloading rate due to wind U_{wind} against wind speed u and (b) snow unloading rate coefficient due to wind f_{wind} against wind speed u. The dashed line in (a) shows $0.61\,\text{mm}\,\text{h}^{-1}$ or the maximum sublimation rate reported by Storck et al. (2002) and the solid line in (b) represents Equation (11). The data were obtained at night with an intercepted snow amount of $\geq 5\,\text{mm}$, an air temperature of $<0°C$, and no precipitation.

FIGURE 7 Scatterplot between modelled and observed (a) snow unloading rate coefficient due to snowmelt f_{melt} (R^2 of 0.78, RMSE of $0.097\,\text{h}^{-1}$) and (b) snow unloading rate coefficient due to wind f_{wind} (R^2 of 0.43, RMSE of $0.025\,\text{h}^{-1}$) for all four snow seasons. The solid line shows a 1:1 relationship.

0.1. These coefficients were smaller relative to the snow unloading rate coefficient due to melt. The obtained snow unloading rate coefficients due to wind included many effects of sublimation. However, the snow unloading rate coefficient due to wind appeared to be increasing with an increase in wind speed, and the following Equation (22) was obtained from these data. The coefficient of determination and the AIC for this regression equation was R^2 of 0.43 and AIC of -486.6, respectively.

$$f_{wind} = 0.020\,u. \qquad (22)$$

3.5 | Model validation

Figure 7a shows the scatterplot between the measured and modelled snow unloading rate coefficient due to snowmelt, and Figure 7b shows the scatterplot due to wind. The RMSE values were 0.097 (h^{-1}) due to snowmelt and 0.025 (h^{-1}) due to wind.

Figure 8 shows the simulated and observed time series of intercepted snow I (mm) during four snow seasons. The intercepted snow was simulated using the developed model of JSIM shown as Equation (8) with the coefficients of $\frac{dI}{dP}$, f_{melt}, and f_{wind}, which were estimated from Equations (20)–(22). The JSIM performed well, and the simulated results were close to the behaviour of the observed
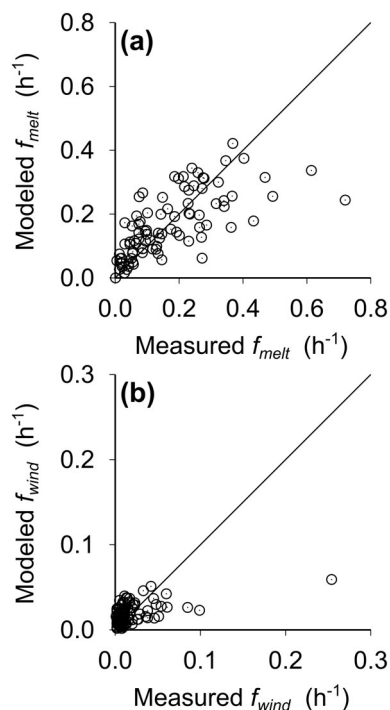
intercepted snow throughout the entire analysis period. However, a large difference of 15–20 mm appeared between the simulated and observed intercepted snow on 17 January 2017; 13 December 2017; 27 December 2017; and 13 February 2018. In all of these cases, the JSIM approximately well simulated the time changes in intercepted snow until the difference between the simulated and observed results began to appear. However, after that, there were times when the model did not correctly simulate the occurrence and amount of snow unloading, as a result, a large difference in the amount of intercepted snow appeared. They occurred during the daytime when the air temperature is around $-2°C$, or during the nighttime when the air temperature is around $0°C$. Figure 9 shows the correlation between the measured and modelled intercepted snow for the entire period of analysis. The statistical measures of the correlation coefficient r, ME, and RMSE for each studied snow season are shown in Table 4. The r for the entire period of analysis was 0.91, which showed a good correlation between the observed and modelled intercepted snow. The ME and RMSE for the entire period of analysis were -0.3 and 2.3 mm, respectively displaying slight underestimates from the JSIM model. The r and RMSE were particularly good in the snow seasons of 2018–2019 ($r = 0.95$, RMSE = 1.7) and 2019–2020 ($r = 0.94$, RMSE = 1.1). During the snow season of 2017–2018, when large differences frequently occurred between the simulated and observed results, the JSIM overestimated the intercepted snow (ME = 0.5), and the r was smallest ($r = 0.87$) as compared to the other seasons.
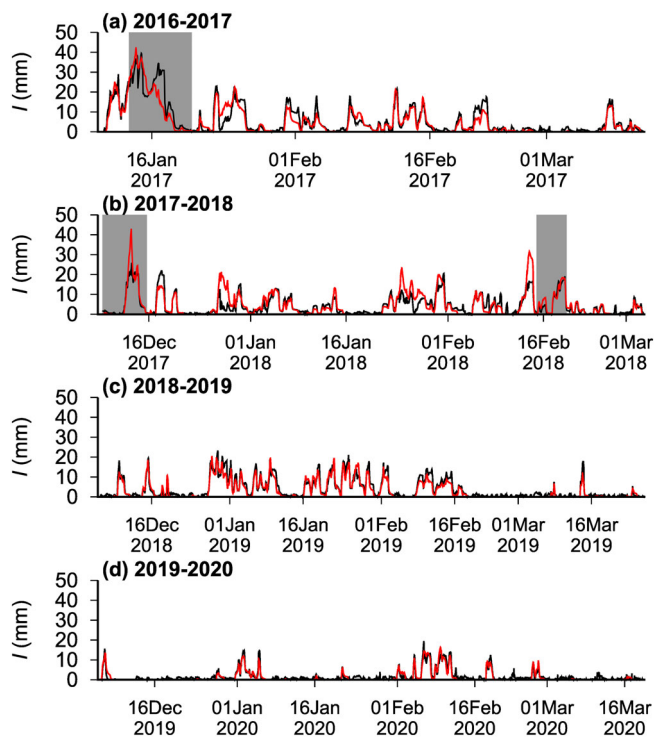
FIGURE 8 Time series of observed and modelled hourly intercepted snow (a) for 2016–2017, (b) for 2017–2018, (c) for 2018–2019, and (d) for 2019–2020. The black line shows the observed hourly intercepted snow, and the red line shows the modelled intercepted snow. Periods shaded in grey indicate periods when data are from a backup precipitation gauge due to equipment malfunction.

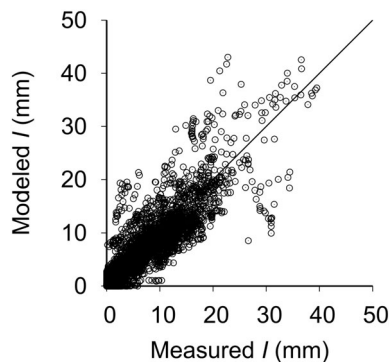**FIGURE 9** Scatterplot between measured and modelled intercepted snow *I* for all four snow seasons. The solid line shows a 1:1 relationship. $r = 0.91$, ME $= -0.3$ mm, and RMSE $= 2.3$ mm for the entire period.

3.6 | Model intercomparison

Figure 10 shows the time series of intercepted snow in the snow season of 2017–2018 simulated by the model in which the snow interception or snow unloading parameterization models are changed from the JSIM to the parameterization models adopted in the other previously developed model, respectively. For intercomparison of snow

TABLE 4 Statistical measures of the correlation coefficient *r*, ME, and RMSE between measured and modelled the interception efficiencies for each study snow season.

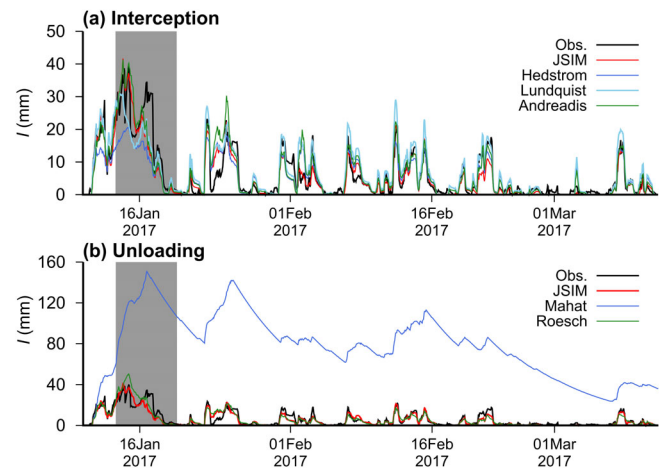| Snow season	r	ME (mm)	RMSE (mm)
2016–2017	0.92	−0.7	3.2
2017–2018	0.87	0.5	3.2
2018–2019	0.95	−0.7	1.7
2019–2020	0.94	−0.4	1.1
All	0.91	−0.3	2.3

FIGURE 10 Time series of observed and simulated hourly intercepted snow using different parameterization models (a) for snow interception model, (b) for snow unloading model. The black line shows the observed hourly intercepted snow, and the red line shows the simulated intercepted snow by JSIM; other coloured lines show the simulated intercepted snow by several models shown in Section 2.6.

interception parameterization, the parameterization model by Hedstrom and Pomeroy (1998), which assumes the exponential curve of intercepted snow growth, underestimated the intercepted snow (RMSE $= 4.4$, ME $= -0.9$). Underestimation was particularly significant during the snow interception event of 10–18 December 2017. The parameterization model by Lundquist et al. (2021), which implements the dependency of maximum interception capacity increases with air temperature increasing, improved the underestimation of intercepted snow by the parameterization model of Hedstrom and Pomeroy (1998) during the snow interception event of 10–18 December 2017. It showed a smaller RMSE than the parameterization model by Hedstrom and Pomeroy (1998); however, it estimated the largest ME of intercepted snow over the entire period than any other models (RMSE $= 3.8$, ME $= 0.8$). The parameterization model by Andreadis et al. (2009), which assumes the constant interception efficiency and the maximum interception capacity depend on air temperature, showed favourable simulated results (RMSE $= 3.7$, ME $= 0.2$) and close behaviour to the simulated results by the JSIM. Comparing the RMSE of these models to that of JSIM (RMSE $= 3.2$, ME $= -0.7$, shown in Table 4), the RMSE of JSIM was the smallest, followed by

the model by Andreadis et al. (2009), Lundquist et al. (2021), and Hedstrom and Pomeroy (1998).

For snow unloading parameterizations, the parameterization by Mahat and Tarboton (2014), which snow unloading is modelled as an exponential function of time, showed significantly overestimated intercepted snow (RMSE = 77.4, ME = 71.7), and the simulated intercepted snow never reached zero throughout the entire period. The parameterization by Roesch et al. (2001), which considers snow unloading doe to melt and wind, showed similar simulated results of the time series of intercepted snow to that of JSIM. However, when snow unloading was observed on 14 January 2017, JSIM evaluated snow unloading, but a parameterization by Roesch et al. (2001) did not assess it. The parameterization by Roesch et al. (2001) showed a larger RMSE for the entire period than the JSIM (RMSE = 4.0, ME = −0.3).

4 | DISCUSSION

4.1 | Interception efficiency

Statistical analysis showed that the interception efficiency at air temperature <0°C tended to increase with increasing air temperature and decrease with increasing wind speed. Similar patterns have been observed in earlier measurements of snow interception on tree canopy (Takahashi, 1952). In prior studies, interception efficiency, determined for each snowfall event in the snow accumulation on a narrow board, increased with an increase in the air temperature >−3°C due to increasing snow cohesion (Kobayashi, 1987; Pfister & Schneebeli, 1999; Takahashi & Takahashi, 1952) and holds constant below −3°C (Kobayashi, 1987). In our experiment, the interception efficiencies were obtained in the air temperature range of −4.2 to 1.3°C, and it is consistent with the transitional air temperature that changes the behaviour of the interception efficiency mentioned in previous studies. However, since only a few data points were obtained at air temperatures <−3°C, it was not possible to determine if the interception efficiency would hold a constant value at air temperatures <−3°C. Takahashi (1952) and Storck et al. (2002) demonstrated that the interception efficiency decreases as wind speed increases due to the snow being removable by the wind. Snow unloading due to wind and sublimation is expected to increase with increasing wind speeds, but these cannot be separated from the observations. It is impossible to determine which is more dominant, but either effect would decrease interception efficiency with increased wind speeds. Alternatively, snow accumulation occurs when snow particles bounce on the snow surface, stop moving, and stay (Kobayashi, 1987). If snow particles are moving at a high velocity before they impact on the snow surface, they are expected to bounce significantly, making snow accumulation less likely to occur. Then, it can be assumed that snow accumulation is less likely to occur due to increased wind velocity, decreasing the interception efficiency.

The observed interception efficiency for air temperature <0°C was constant with increasing of the amount of intercepted snow. It had no statistically significant relationship to the amount of intercepted snow. This is similar to the results of warmer maritime climates shown by Storck et al. (2002) and Roth and Nolin (2019). If it can be assumed that the amount of intercepted snow increases with increasing cumulative snowfall precipitation and that there is an asymptotic change approaching the maximum interception capacity as represented by a sigmoidal or exponential curve, then the interception efficiency would be expected to be not constant with increasing intercepted snow. The result indicates that within the measured range of the intercepted snow amount, the maximum interception capacity does not exist, or it is sufficiently large to have no impact on the interception efficiency. This is most likely due to the air temperature at the time of snowfall. At temperatures >−3°C, the angle of repose for snow reaches 90° (Eidevåg et al., 2022; Kuroiwa et al., 1967), and the snow accumulation on objects is expected to grow vertically, maintaining its initial shape of the object's projection. In such cases, accumulated snow will continue to grow with continued snowfall, and the maximum capacity of accumulated snow will not appear unless broken by external forces. Suppose this same behaviour occurs in snow accumulation on the tree canopy. In that case, the maximum interception capacity is not expected to appear, and the interception efficiency does not change with increasing cumulative snowfall precipitation. On the other hand, it is not certain whether the maximum interception capacity exists at air temperatures <−4°C, which is lower than the temperature we observed. The angle of repose for snow particles tends to rapidly decrease with a decrease in air temperature under −3.5°C (Eidevåg et al., 2022; Kuroiwa et al., 1967). From data obtained during nine storm events at air temperatures ranging from −12.1 to −1.9°C, Moeser et al. (2015) suggested that the interception efficiency increases with increasing event precipitation and decreases after the interception efficiency reached maximum value. This suggests the existence of a maximum interception capacity under colder conditions.

The interception efficiency for air temperature ≥0°C tended to decrease with increasing air temperature and amount of intercepted snow. At temperatures ≥0°C, snow particles partially melt during their fall and contain water. The liquid water fraction of a snow particle relates to air temperature, relative humidity, and precipitation rate (Misumi et al., 2014). As air temperature increases, the fraction of liquid water contained in the snowfall particles increases, while the amount of solid precipitation decreases. As a result, it is assumed that even if the same amount of precipitation occurs, higher temperatures will reduce the amount of snow supplied on the tree canopy, corresponding to a decrease in the interception efficiency. Furthermore, melting of intercepted snow is likely to occur at air temperatures ≥0°C. Equation (10) shows that snow unloading due to snowmelt can occur even at nighttime if the air temperature is >0°C. However, in our measurements, the obtained interception efficiency unavoidably includes the effect of snow unloading. Based on these considerations, if the amount of intercepted snow is large, it is assumed that the snow unloading rate due to snowmelt will also be large, decreasing the interception efficiency as intercepted snow increases. In contrast, as shown in Figure 3b, the interception efficiency appears low when the

amount of intercepted snow is less than 5 mm. At this experimental site, air temperatures are often higher in the early stages of a snowfall event, and it decreases with time. Figure 11 shows the relationship between air temperature and the amount of intercepted snow when the interception efficiency is observed. In order to discuss the effect of the air temperature at the early stages of a snowfall event on the interception efficiency when snowfall occurs at temperatures ≥0°C, we will take a typical example of intercepted snow of 0 and 5 mm. As Figure 11 shows, when the amount of intercepted snow is 0 and 5 mm, the mean air temperature at the time the interception efficiency data were observed is approximately 0.5 and 0.2°C, respectively. According to Equation (20), the change in interception efficiency due to the difference in the air temperature is estimated to be 0.18 lower when the air temperature is 0.3°C higher. In Figure 3b, the mean interception efficiency is 0.39 for intercepted snow of 0 mm and 0.62 for 5 mm, respectively. The difference is 0.23, which is approximately the same as the difference in interception efficiency due to air temperature differences determined from Equation (20). It seemed that the difference in the interception efficiency under these two conditions is mainly caused by the difference in air temperature. Therefore, it is assumed that the smaller interception efficiency for the amount of intercepted snow <5 mm was influenced by the higher air temperature during the early stages of the snowfall event, and it is not due to the sigmoidal curve behaviour of intercepted snow growth.

The coefficient of determination R^2 and RMSE between the measured and modelled interception efficiency were 0.38, and 0.20, respectively at air temperature ≥0°C and 0.16, and 0.21, respectively at air temperature <0°C. The results show that the modelled interception efficiency is uncertain, and the explanatory variables used in this analysis do not fully explain the interception efficiency. Schmidt and Gluns (1991) demonstrated that the bouncing of snow particles increased as the new snow density increased, reducing the amount of interception. New snow density relates to the dominant shapes of crystals (Ishizaka et al., 2016), and the fall speed of snow particles relates to the dominant shapes of crystals (Locatelli & Hobbs, 1974). These findings indicate that air temperature and wind speed alone is insufficient for modelling the interception efficiency and that
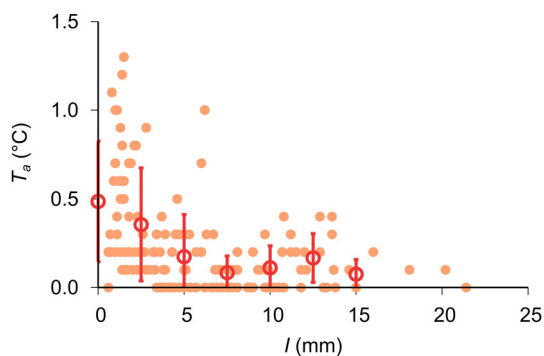
information about snowfall particles may improve the prediction accuracy of interception efficiency.

4.2 | Snow unloading

For snow unloading due to snowmelt, the coefficients of determination for the linear regression analysis with a single explanatory variable were the largest for solar radiation, followed by intercepted snow quantity, and the smallest for the air temperature. Multiple regression analysis yielded the best regression model using all three of these variables. The snow unloading rate coefficient due to snowmelt f_{melt} is related to the amount of snowmelt. Therefore, we consider the implications of the best regression model obtained from the energy balance of a snow-covered canopy. The albedo of snow-covered canopies is low (<0.2), and the net radiation above the canopy during the daytime remains positive (Pomeroy & Dion, 1996). The net radiation is greater than the sensible heat flux, and it is dominant for energy balance above the canopy (Nakai et al., 1999). When the air temperatures is slightly above 0°C where snow unloading was mainly observed, the sensible heat is small, and the effect of air temperature on the snow unloading due to snowmelt is considered smaller than the effect of solar radiation. Furthermore, snowmelt-induced mass releases cause a significant amount of intercepted snow to be removed from the canopy all at once. During such a snow large unloading event, the unloading snow induces further unloading in the lower canopy (Takahashi, 1952). The magnitude of the impact force seemed to be related to the mass of the intercepted snow released at one time. The existence of a correlation between the unloading rate coefficient and the amount of intercepted snow may be related to such a falling snow phenomenon. Therefore, in modelling the snow unloading rate coefficient due to snowmelt, it is not sufficient to use only air temperature as an explanatory variable. The solar radiation and the amount of intercepted snow should also be considered. It is the only snow interception model to take account the effect of solar radiation in the snow unloading parameterization. In this experiment, the snow unloading rate coefficient due to snowmelt was modelled using a cut tree set up in an open area that was exposed to greater solar radiation than the forest tree canopy. The canopy structure and solar angle affect shortwave transmissivity through the canopy and the net radiation above the canopy (Pomeroy & Dion, 1996). As a result, when Equation (22) is adapted to the simulation of the intercepted snow on the forest canopy, the parameters may need to be adjusted to account for the tree species and the canopy structure.

Snow unloading due to wind, which exceeded the maximum sublimation rates observed in previous studies, began to appear at wind speeds above 0.8 m s^{-1}. The snow unloading rate coefficient due to wind increased with increasing wind speed. These results are similar to those observed by Takahashi (1952). However, only a few data were identifiable as the snow unloading due to wind, and most data could not distinguish whether it is caused by the snow unloading due to wind or sublimation. Most of these may represent a decrease in intercepted snow due to sublimation. These results suggest that the

FIGURE 11 Scatter plot and binned scatter plot air temperature T_a of against intercepted snow I when the interception efficiency is observed at air temperature $T_a \geq 0°C$. The open circles are the means within each bin and the error bars represent the standard deviations.

snow unloading due to wind is smaller than the sublimation rate or does not occur in such a range of wind speeds. For these reasons, Equation (22) does not appear to accurately describe wind-driven unloading. An observation method that exactly separates the snow unloading due to wind or sublimation is necessary to improve our understanding and modelling of these phenomena.

4.3 | Model validation and intercomparison

Although the modelled interception efficiency contains high uncertainty, the simulated behaviour of intercepted snow had a good correlation coefficient of 0.91 and RMSE of 2.3 mm for the entire analysis period. From the intercomparison results for snow interception, the JSIM simulated the time series of intercepted snow better than the model by Andreadis et al. (2009), which assumes a constant snow interception efficiency regardless of air temperature, or the model by Hedstrom and Pomeroy (1998) or Lundquist et al. (2021), which assumes the exponential curve of intercepted snow growth and the maximum interception capacity increases with air temperature increases. The means of observed interception efficiencies shown in Figure 3 were 0.54 for air temperatures of ≥0°C and 0.63 for air temperatures <0°C, similar to 0.6 adopted in the model of Andreadis et al. (2009). Statistical analysis shows that interception efficiency varies with air temperature. Since the JSIM employed a parameterization model that expresses interception efficiency as a function of air temperature, the JSIM seems to estimate better the time series of intercepted snow than the model of Andreadis et al. (2009). In addition, the observed results of snow interception efficiency do not show an asymptotic change in the intercepted snow approaching the maximum interception capacity, as represented by the sigmoidal or exponential curves. These facts may indicate that a snow interception parameterization in which the snow interception efficiency increases with increasing air temperature is appropriate for simulating snow interception phenomena in warmer regions like those in this study. We do not recommend, but suppose, a snow interception parameterization that assumes the sigmoidal or exponential curve of intercepted growth will be used to simulate intercepted snow in warmer regions. In that case, the parameterization model should include the effect of increasing maximum interception capacity and interception efficiency due to increasing air temperature for air temperature >−3°C, and its model parameters should be chosen carefully.

From the intercomparison results for snow unloading, the model by Mahat and Tarboton (2014), which represents snow unloading as a function of time, significantly overestimated the intercepted snow for the entire period. The model was developed for cold boreal forests where snow unloading due to snow melt is insignificant. The results indicate that it is not appropriate to adapt this model to warmer regions where snowmelt frequently occurs during winter. The JSIM or model by Roesch et al. (2001), which incorporates snow unloading due to snow melt, produced simulated results close to the observed intercepted snow time series. The model represents snow unloading due to snow melt would be particularly effective in modelling snow

interception in warm regions where snow melt is significant during winter. The JSIM produced better-simulated results of intercepted snow close to observations than the model by Roesch et al. (2001), which uses only air temperature to represent snow unloading due to snow melt. It indicates that the model can be improved by incorporating the effect of solar radiation into a parameterization model of snow unloading due to snow melt.

However, 15–20 mm difference appeared between the simulated by the JSIM and observed intercepted snow in some snowfall events. These occurred during the daytime when the air temperature was around −2°C or during the nighttime when the air temperature was around 0°C. These conditions correspond to the boundaries that are likely to start snow unloading due to snowmelt. Therefore, it is assumed that snowmelt initiated the snow unloading errors. It seems that the miss estimation of snow unloading occurring by the model is sensitive to the simulation results of the amount of intercepted snow. To obtain favourable simulated results, both the snow accumulation and snow unloading schemes must work properly. This is especially important in simulating the temporal change of intercepted snow in warmer regions where snowmelt is more likely to occur. Because snowmelt causes a mass release of intercepted snow, misestimation of snow unloading due to snowmelt can lead to critical errors in the simulation of intercepted snow. Thus, careful considerations will be needed to develop a model that represents snow unloading due to snowmelt and to determine its model parameters.

In this study, the snow interception phenomena have been discussed without regard to the effects of canopy structure. Recent observations suggested that the forest canopy structure influences interception efficiency (Moeser et al., 2015; Roth & Nolin, 2019). Snow interception is probably impacted because canopy structure affects microclimate, such as wind speed and solar radiation within the canopy. Canopy structure may help distribute point-based models to the surrounding forest landscape. Future testing of the developed model using data observed in different meteorological conditions and forest canopy structures is needed to improve the model and better understand the snow interception phenomenon.

5 | CONCLUSIONS

A new parameterization model, which represents snow interception and unloading, was developed based on observed results. A weighing tree experiment using cut cedar trees investigated the relationship between meteorological conditions and intercepted snow on the tree canopy at Tokamachi, which located in a relatively warm and snow rich area in Japan. The interception efficiency at air temperatures <0°C increased with increasing air temperature and decreasing wind speed. It was not related to the amount of intercepted snow, and the maximum interception capacity was not present at air temperatures from −4.2 to 0°C. Due to a lack of data, it was not possible to show whether the maximum interception capacity existed at temperatures <−3°C. At air temperatures ≥0°C, the interception efficiency decreased with increasing air temperature

and the amount of intercepted snow. The snow unloading due to snowmelt was related to air temperature, solar radiation, and the amount of intercepted snow. The snow unloading caused by wind-blowing intercepted snow off the tree, started to develop at wind speeds exceeding 0.8 m s^{-1}. The snow unloading rate due to wind increased with increasing wind speed. The simulated temporal changes of intercepted snow were close to the observed ones. A difference of 15–20 mm due to snow unloading errors appeared between the simulated and observed intercepted snow on some snowfall events. Future testing for colder meteorological conditions and different forest canopy structures must confirm the adaptability of the developed model to them.

ACKNOWLEDGEMENTS

CONFLICT OF INTEREST STATEMENT

The authors declare no conflict of interest.

DATA AVAILABILITY STATEMENT

The data supporting the findings of this study are available upon request from the corresponding author.

ORCID

Takafumi Katsushima https://orcid.org/0000-0002-7770-313X
Kazuki Nanko https://orcid.org/0000-0002-1157-9287
Shigeki Murakami https://orcid.org/0000-0002-4193-055X

REFERENCES

Andreadis, K. M., Storck, P., & Lettenmaier, D. P. (2009). Modelling snow accumulation and ablation processes in forested environments. *Water Resources Research*, *45*, W05429. https://doi.org/10.1029/2008WR007042

Betts, A. K., & Ball, J. H. (1997). Albedo over the boreal forest. *Journal of Geophysical Research*, *102*(D24), 28901–28909. https://doi.org/10.1029/96JD03876

Davenport, A., Grimmond, C., Oke, T., & Wieringa, J. (2000). Estimating the roughness of cities and sheltered country. *Paper presented at 15th conference on probability and statistics in the atmospheric sciences/12th conference on applied climatology*, American Meteorological Society, Ashville, NC (pp. 96–99).

Eidevåg, T., Thomson, E. S., Kallin, D., Casselgren, J., & Rasmuson, A. (2022). Angle of repose of snow: An experimental study on cohesive properties. *Cold Regions Science and Technology*, *194*, 103470. https://doi.org/10.1016/j.coldregions.2021.103470

Goodison, B., Louie, P., & Yang, D. (1998). *WMO solid precipitation measurement intercomparison: Final report. Instruments and observing methods report, 67 (WMO/TD No. 872)*. World Meteorological Organization Publications.

Gregow, H., Venäläinen, A., Peltola, H., Kellomäki, S., & Schultz, D. (2008). Temporal and spatial occurrence of strong winds and large snow load amounts in Finland during 1961–2000. *Silva Fennica*, *42*(4), 515–534. https://doi.org/10.14214/sf.231

Hedstrom, N. R., & Pomeroy, J. W. (1998). Measurements and modelling of snow interception in the boreal forest. *Hydrological Processes*, *12*, 1611–1625. https://doi.org/10.1002/(SICI)1099-1085(199808/09)12:10/11<1611::AID-HYP684>3.0.CO;2-4

Helbig, N., Moeser, D., Teich, M., Vincent, L., Lejeune, Y., Sicart, J.-E., & Monnet, J.-M. (2020). Snow processes in mountain forests: Interception modeling for coarse-scale applications. *Hydrology and Earth System Sciences*, *24*, 2545–2560. https://doi.org/10.5194/hess-24-2545-2020

Ishizaka, M., Motoyoshi, H., Yamaguchi, S., Nakai, S., Shiina, T., & Muramoto, K. (2016). Relationships between snowfall density and solid hydrometeors, based on measured size and fall speed, for snowpack modeling applications. *The Cryosphere*, *10*, 2831–2845. https://doi.org/10.5194/tc-10-2831-2016

Kato, A. (2000). *Study on the approach for estimating resistance of Japanese cedar to snow accretion damage and its application* (Doctoral dissertation). Iwate University, Iwate. Retrieved from CiNii. https://ci.nii.ac.jp/naid/500000191577

Kobayashi, D. (1987). Snow accumulation on a narrow board. *Cold Regions Science and Technology*, *13*(3), 239–245. https://doi.org/10.1016/0165-232X(87)90005-X

Kuroiwa, D., Mizuno, Y., & Takeuchi, M. (1967). Micromeritical properties of snow. *Paper presented at international conference on low temperature science, physics of snow and ice* (Vol. 1(2), pp. 751–772).

Liston, G. E., & Elder, K. (2006). A distributed snow-evolution modelling system (SnowModel). *Journal of Hydrometeorology*, *7*(6), 1259–1276. https://doi.org/10.1175/JHM548.1

Locatelli, J. D., & Hobbs, P. V. (1974). Fall speeds and masses of solid precipitation particles. *Journal of Geophysical Research*, *79*, 2185–2197. https://doi.org/10.1029/JC079i015p02185

Lumbrazo, C., Bennett, A., Currier, W. R., Nijssen, B., & Lundquist, J. (2022). Evaluating multiple canopy-snow unloading parameterizations in SUMMA with time-lapse photography characterized by citizen scientists. *Water Resources Research*, *58*, e2021WR030852. https://doi.org/10.1029/2021WR030852

Lundberg, A., & Halldin, S. (1994). Evaporation of intercepted snow: Analysis of governing factors. *Water Resources Research*, *30*(9), 2587–2598. https://doi.org/10.1029/94WR00873

Lundquist, J. D., Dickerson-Lange, S., Gutmann, E., Jonas, T., Lumbrazo, C., & Reynolds, D. (2021). Snow interception modelling: Isolated observations have led to many land surface models lacking appropriate temperature sensitivities. *Hydrological Processes*, *35*(7), e14274. https://doi.org/10.1002/hyp.14274

Mahat, V., & Tarboton, D. G. (2014). Representation of canopy snow interception, unloading and melt in a parsimonious snowmelt model. *Hydrological Processes*, *28*(26), 6320–6336. https://doi.org/10.1002/hyp.10116

Masuda, A., Itado, A., Taniguchi, K., Sakai, K., Uyeda, H., Yamashita, K., & Nakai, S. (2018). Improving of winter quantitative precipitation estimation using XRAIN. *Journal of Japan Society of Civil Engineers, Series B1 (Hydraulic Engineering)*, *74*(4), 85–90. https://doi.org/10.2208/jscejhe.74.I_85

Miller, D. H. (1966). *Transport of intercepted snow from trees during snow storms. (Res. Paper PSW-RP-033)*. U.S. Department of Agriculture, Forest Service, Pacific Southwest Forest & Range Experiment Station.

Misumi, R., Motoyoshi, H., Yamaguchi, S., Nakai, S., Ishizaka, M., & Fujiyoshi, Y. (2014). Empirical relationships for estimating liquid water fraction of melting snowflakes. *Journal of Applied Meteorology and Climatology*, *53*(10), 2232–2245. https://doi.org/10.1175/JAMC-D-13-0169.1

Moeser, D., Mazotti, G., Helbig, N., & Jonas, T. (2016). Representing spatial variability of forest snow: Implementation of a new interception model. *Water Resources Research*, *52*, 5041–5059. https://doi.org/10.1002/2015WR017961

Moeser, D., Stähli, M., & Jonas, T. (2015). Improved snow interception modelling using canopy parameters derived from airborne LiDAR data. *Water Resources Research*, *51*(7), 5041–5059. https://doi.org/10.1002/2014wr016724

Nakai, Y., Sakamoto, T., Terajima, T., Kitahara, H., & Saito, T. (1994). Snow interception by forest canopies: Weighing a conifer tree with meteorological observation and analysis with Penman-Monteith formula. *IAHS Publication*, *223*, 227–236.

Nakai, Y., Sakamoto, T., Terajima, T., Kitamura, K., & Shirai, T. (1999). The effect of canopy-snow on the energy balance above a coniferous forest. *Hydrological Processes*, *13*, 2371–2382. https://doi.org/10.1002/(SICI)1099-1085(199910)13:14/15%3C2371::AID-HYP871%3E3.0.CO;2-1

Pfister, R., & Schneebeli, M. (1999). Snow accumulation on boards of different sizes and shapes. *Hydrological Processes*, *13*, 2345–2355. https://doi.org/10.1002/(SICI)1099-1085(199910)13:14/15<2345::AID-HYP873>3.0.CO;2-N

Pomeroy, J. W., & Dion, K. (1996). Winter radiation extinction and reflection in a boreal pine canopy: Measurements and modelling. *Hydrological Processes*, *10*, 1591–1608. https://doi.org/10.1002/(SICI)1099-1085(199612)10:12<1591::AID-HYP503>3.0.CO;2-8

Roesch, A., Wild, M., Gilgen, H., & Ohmura, A. (2001). A new snow cover fraction parametrization for the ECHAM4 GCM. *Climate Dynamics*, *17*, 933–946. https://doi.org/10.1007/s003820100153

Roth, T. R., & Nolin, A. W. (2019). Characterizing maritime snow canopy interception in forested mountains. *Water Resources Research*, *55*, 4564–4581. https://doi.org/10.1029/2018WR024089

Satterlund, D. R., & Haupt, H. F. (1967). Snow catch by conifer crowns. *Water Resources Research*, *3*, 1035–1039. https://doi.org/10.1029/WR003i004p01035

Schmidt, R. A., & Gluns, D. R. (1991). Snowfall interception on branches of three conifer species. *Canadian Journal of Forest Research*, *21*, 1262–1269. https://doi.org/10.1139/x91-176

Schmidt, R. A. (1991). Sublimation of snow intercepted by an artificial conifer. *Agricultural and Forest Meteorology*, *54*(1), 1–27. https://doi.org/10.1016/0168-1923(91)90038-R

Storck, P. (2000). *Trees, snow and flooding: An investigation of forest canopy effects on snow accumulation and melt at the plot and watershed scales in the Pacific northwest. Water resources series technical reports*, *161*. University of Washington.

Storck, P., Lettenmaier, D. P., & Bolton, S. M. (2002). Measurement of snow interception and canopy effects on snow accumulation and melt in a mountainous maritime climate, Oregon, United States. *Water Resources Research*, *38*(11), 5-1–5-16. https://doi.org/10.1029/2002WR001281

Takahashi, K. (1952). Snow-crown on Japanese cedar tree (in Japanese, Authors translated the title). Study of the fallen snow on the forest trees (the first report). *Bulletin of the Government Forest Experiment Station*, *54*, 140–148.

Takahashi, T., & Takahashi, K. (1952). Size of future and snow accumulation, mechanism of snow accumulation on a narrow board (in Japanese, Authors translated the title). Study of the fallen snow on the forest trees (the first report). *Bulletin of the Government Forest Experiment Station*, *54*, 117–121.

Takeuchi, Y., Endo, Y., & Niwano, S. (2016). Estimation of solid and liquid precipitations categorized based on air temperature during snowfall or rainfall. *Bulletin of FFPRI*, *15*(4), 145–149. https://doi.org/10.20756/ffpri.15.4_145

Tamura, M. (1993). An automatic system for controlling snow on roofs. *Annals of Glaciology*, *18*, 113–116. https://doi.org/10.3189/S0260305500011356

Yamazaki, T., Fukabori, K., & Kondo, J. (1996). Albedo of forest with crown snow. *Seppyo*, *58*(1), 11–18. https://doi.org/10.5331/seppyo.58.11

Yokoyama, K., Ohno, H., Kominami, Y., Inoue, S., & Kawakata, T. (2003). Performance of Japanese precipitation gauges in winter. *Seppyo*, *65*(3), 303–316. https://doi.org/10.5331/seppyo.65.303

Yoshida, S., & Saito, K. (1956). Some experiments on totalizers. *Seppyo*, *17*(2), 8–13. https://doi.org/10.5331/seppyo.17.2_8